sustainability

MDPI

Article

Low-Cost and Contactless Survey Technique for Rapid Pavement Texture Assessment Using Mobile Phone Imagery

Zhenlong Gong [1,2], Marco Bruno [2], Margherita Pazzini [2,*], Anna Forte [2], Valentina Alena Girelli [2], Valeria Vignali [2] and Claudio Lantieri [2]

[1] National Center for Materials Service Safety, University of Science and Technology Beijing, Beijing 100083, China; zhenlong.gong@unibo.it
[2] Department of Civil, Chemical, Environmental and Material Engineering (DICAM), University of Bologna, 40136 Bologna, Italy; marco.bruno14@unibo.it (M.B.); anna.forte3@unibo.it (A.F.); valentina.girelli@unibo.it (V.A.G.); valeria.vignali@unibo.it (V.V.); claudio.lantieri2@unibo.it (C.L.)
* Correspondence: margherita.pazzini2@unibo.it

Abstract: Collecting pavement texture information is crucial to understand the characteristics of a road surface and to have essential data to support road maintenance. Traditional texture assessment techniques often require expensive equipment and complex operations. To ensure cost sustainability and reduce traffic closure times, this study proposes a rapid, cost-effective, and non-invasive surface texture assessment technique. This technology consists of capturing a set of images of a road surface with a mobile phone; then, the images are used to reconstruct the 3D surface with photogrammetric processing and derive the roughness parameters to assess the pavement texture. The results indicate that pavement images taken by a mobile phone can reconstruct the 3D surface and extract texture features with accuracy, meeting the requirements of a time-effective documentation. To validate the effectiveness of this technique, the surface structure of the pavement was analyzed in situ using a 3D structured light projection scanner and rigorous photogrammetry with a high-end reflex camera. The results demonstrated that increasing the point cloud density can enhance the detail level of the real surface 3D representation, but it leads to variations in road surface roughness parameters. Therefore, appropriate density should be chosen when performing three-dimensional reconstruction using mobile phone images. Mobile phone photogrammetry technology performs well in detecting shallow road surface textures but has certain limitations in capturing deeper textures. The texture parameters and the Abbott curve obtained using all three methods are comparable and fall within the same range of acceptability. This finding demonstrates the feasibility of using a mobile phone for pavement texture assessments with appropriate settings.

Keywords: pavement texture assessment; close-range photogrammetry; structured-light scanner; 3D image analysis; sustainable road maintenance

Citation: Gong, Z.; Bruno, M.; Pazzini, M.; Forte, A.; Girelli, V.A.; Vignali, V.; Lantieri, C. Low-Cost and Contactless Survey Technique for Rapid Pavement Texture Assessment Using Mobile Phone Imagery. *Sustainability* **2024**, *16*, 9630. https://doi.org/10.3390/su16229630

Academic Editors: Miguel Sol-Sánchez, Davide Lo Presti, Giuseppe Sollazzo and Kelvin CP Wang

Received: 7 September 2024
Revised: 19 October 2024
Accepted: 31 October 2024
Published: 5 November 2024

1. Introduction

Pavement texture, as a key indicator of pavement structure, has a direct impact on driving safety, driving comfort, noise levels, and pavement durability [1–4]. Specifically, the roughness of pavement texture affects the grip of tires, which, in turn, affects the braking performance and handling of vehicles [5–7]. In addition, good pavement texture can effectively reduce the risk of skidding by effectively removing water from the road surface, as well as improve driving comfort by absorbing the noise generated between tires and the road surface [8–10]. Therefore, the accurate acquisition and assessment of pavement texture is crucial for road maintenance and management. Traditional pavement texture test methods often use the sand patch method, which is a contact-based approach that is prone to human error [11–13]. However, this method has certain drawbacks, such as the potential for sand residues to remain on the analyzed road surface. Furthermore, it necessitates the

interruption of vehicular traffic during testing, which can be disruptive and impractical in high-traffic areas. Thus, non-contact detection technologies have been developed, such as laser scanners, structured-light projection 3D scanners, and high-end reflex cameras [14–18]. These non-contact test methods rely heavily on precision instrumentation. These devices can provide highly accurate measurements, but they are expensive to use and complicated to operate. For example, laser and 3D scanners require professional personnel to operate, and traffic often needs to be closed to conduct tests [19]. While high-end reflex cameras can provide high-resolution images, they are more expensive compared to mobile phones and require time-consuming procedures to collect data [20]. These traditional methods are often incompatible with the need for rapid surveys and timely road reopening, which are essential for properly managing and monitoring pavement conditions.

With the rapid development of mobile devices and image processing technology, using portable devices such as mobile phones for 3D reconstruction has become a new research topic [21–23]. Mobile phones are equipped with high-resolution cameras and powerful computing capabilities, making it possible to achieve 3D reconstruction based on mobile phone imagery [24]. Photogrammetry using mobile phones has achieved remarkable results in fields such as geological exploration and tunnel measurement. Fang et al. [25] used multiple mobile phone images to reconstruct a 3D model of a tunnel, obtaining an error margin within 0.3 cm. Similarly, Fang et al. [26] employed a similar strategy to monitor rock slopes, by effectively analyzing rock deformation behavior and failure mechanisms. These studies show that photogrammetry is highly reliable and applicable in reconstructing complex terrains and structures. Mobile phone images can be used not only for the 3D reconstruction of geological structures but also for reconstructing coarse particles. An et al. [27] quickly determined particle size and shape through mobile phone photogrammetry, indicating that photogrammetry can be applied to smaller areas for texture analysis, thus providing the potential for pavement texture reconstruction. Wan et al. [28] used three different mobile phones and image processing technologies to obtain concave distribution characterization of the pavement, which can effectively reflect the segregation condition of the pavement surface. Slavkovic and Bjelica [29] also extracted pavement texture features from the image. However, their analysis was not conducted by transforming the photo into a 3D point cloud. Farhadmanesh et al. [30] used mobile photogrammetry to reconstruct the pavement for pavement crack assessment, but the error reached 1 cm, and accuracy could not be used for texture assessment. Kogbara et al. [31] attempted to reconstruct pavement in 3D and evaluate pavement texture using a professional full-frame DSLR camera with success, but the camera body alone is costly. These studies suggest that photogrammetry has significant potential in assessing road pavement texture, particularly in monitoring and asset management contexts, as it can reduce both costs and road closure times when evaluating the efficacy of maintenance interventions. Moreover, using mobile phones for this purpose is feasible and can further reduce equipment-related costs. Although existing research indicates that photogrammetry based on mobile phone images hold significant potential in pavement texture assessments, current technological methods still have notable limitations. Factors such as the shooting angle, distance, and algorithm for reconstruction greatly affect the 3D reconstruction results [27,32,33]. Additionally, the low resolution of mobile phone images makes it difficult to achieve detailed measurements [34,35].

In response to these issues, this study proposes an innovative and standardized method for evaluating pavement texture based on mobile phone images and photogrammetry. This method is characterized by its speed, cost-effectiveness, and non-invasiveness, making it suitable for various application scenarios. Its accelerated process reduces road closure times compared to traditional, point-based tests, cutting costs and minimizing disruptions. Using a mobile phone with a camera, the method is cost-effective while still providing data quality comparable to more expensive equipment. Environmentally, it minimizes waste generation and simplifies waste management.

Firstly, to improve the reliability of the assessment, a standardized shooting platform was developed that stabilizes the shooting distance, minimizing the impact of environmental factors and human error on the 3D reconstruction process. Then, the effect of the number of point clouds on the texture parameters and computational speed were compared, in order to select the appropriate point cloud density. Finally, a comparative analysis of various techniques was performed by analyzing the Abbott curves and various texture parameters to demonstrate the reliability and practicality of the method based on mobile phone imagery. Additionally, tests were also carried out on pavements with water residue to determine the feasibility of the method in complicated environments.

2. Materials

In this study, a new thin layer of asphalt concrete measuring 20 m × 4 m (80 m^2) with a thickness of 5 cm was placed on the existing pavement in a parking area located at Autodromo Enzo and Dino Ferrari of Imola. A layer of bitumen emulsion was laid to ensure continuity between the two pavement surface layers. The asphalt mixture was made by traditional unmodified bitumen (50/70) with aggregates (passing through a 12.5 mm sieve) at approximately 160 °C. The pavement grading curve is shown in Figure 1. After laying, core samples were taken from the pavement to test the basic performance of the asphalt mixture and its constituent materials. The characteristic of the newly laid asphalt concrete are shown in Table 1.

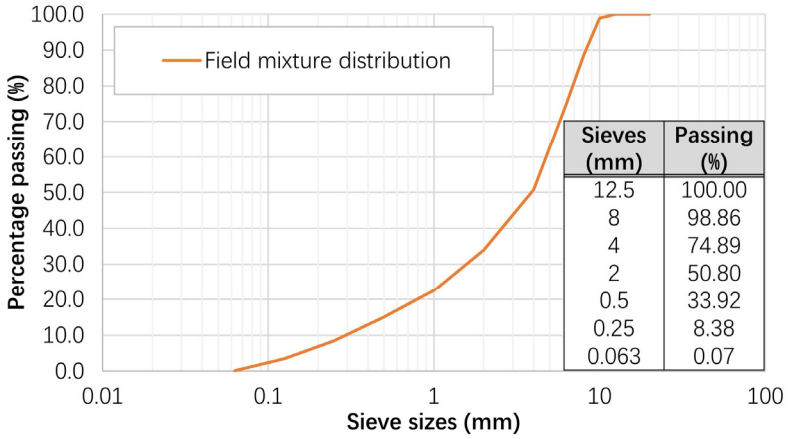

Figure 1. Asphalt mixture grading curves.

Table 1. The basic performance of the asphalt mixture and its constituent materials.

Density ($g \cdot cm^{-3}$)			Percentage of Bitumen (%)	Percentage of Filler (%)
Aggregates	**Bitumen**	**Asphalt Mixture**		
2.651	1.025	2.455	5.73	6.08

3. Methods

3.1. Close-Range Photogrammetry Based on Mobile Phone

Close-range photogrammetry (CRP) is a technique used to reconstruct the three-dimensional shape and structure by capturing multiple photos of the object from different angles. The overall workflow of CRP is shown in Figure 2. The first step is image acquisition, and the quality of the images directly affects the quality of the 3D reconstruction. The quality of the images depends on the tools used for capturing them, the settings of the relevant parameters, and the surveyor skills. In this study, a mobile phone with a Sony IMX315 CMOS (Complementary Metal-Oxide-Semiconductor) sensor with a diagonal of 6.15 mm, an image resolution of 4032 × 3024 pixels, and a pixel size of 1.22 µm was chosen as the camera tool. A sensor is a type of image sensor used in digital cameras, converting

light into electronic signals to create digital images. CMOS sensors are known for their high image quality and low noise levels, which are crucial for capturing detailed and high-resolution images that can improve the quality of the photogrammetric reconstruction. The camera settings were as follows: no zoom, portrait mode, 3 s selfie timer, f/10 aperture, and focus on the specimen (black object). To reduce the impact of manual operation on image quality, two shooting platforms were designed on which the mobile phone was placed to avoid issues like shaking and shooting distance. The shooting strategy is another factor affecting the quality of the 3D point cloud. The strategy used in this study is convergent axis capture, with circular shooting at two different heights. The schematic diagram is shown in Figure 3a. The heights of the platforms were set at 50 cm and 30 cm from the ground to ensure consistent shooting distances. The use of different acquisition heights and angles is crucial in photogrammetric data acquisition, for these main reasons:

- Overall Scene Coverage and Detailed data capture: Capturing images from a higher elevation allows us to obtain "framing" shots that include the entire pavement area. These images ensured that the full extent of the scene was covered, providing context and spatial reference for the detailed images. In contrast, images taken from a lower elevation focused on close-up details of the pavement surface. These images captured finer textures and small-scale features that may not be resolved in the images acquired from higher viewpoints. In fact, the spatial resolution of the images (or Ground Sampling Distance, GSD) was affected by the camera–object acquisition distance (d_o) and focal length (f), as stated by the formula:

$$\text{GSD} = \frac{d_o \times \text{Pixel Size}}{f}$$

  Therefore, the closer the camera is to the surveyed object, the smaller the Ground Sampling Distance (GSD) value will be. A smaller GSD means that each pixel in the digital image represents a shorter distance on the physical object, allowing finer details to be captured.
- Enhanced Robustness of Photogrammetric Reconstruction: combining images from different heights and angles improves the robustness of the image acquisition scheme for 3D reconstruction with photogrammetry. The different perspectives increase image overlap and parallax, which enhance feature matching and tie-point generation during Structure-from-Motion photogrammetry processing. Shooting at multiple tilts and angles, in addition, enables a better completeness of the information captured in the images. However, for this initial test, only nadiral (or images captured perpendicularly to the main surface of interest) were collected.

A height of 50 cm can provide good image overlap, while a height of 30 cm allows for better detail capture with sufficient overlap. While capturing images, both shooting platforms were rotated to ensure that images were taken from different angles. The shooting platforms are shown in Figure 3b. To capture finer details, after rotating the 30 cm platform for a full circle, horizontal movement shooting was conducted.

The second step in CRP is 3D reconstruction, which depends on the algorithms and computational power. In this study, the Structure from Motion (SfM) software 3DF Zephyr (v. 6.509) was used for reconstruction because its Samantha and Stasia algorithms are more suitable for architecture and urban monitoring [36]. Regarding computational power, a laptop was used for this study. The reconstruction of the dense 3D point cloud typically takes less than 10 min, meeting the computational requirements. The 3D reconstruction process first determines the relative positions and orientations of the cameras based on feature points. In Figure 2, the blue conical shapes represent the relative positions of the cameras, which are mainly distributed on both layers in a circular pattern, corresponding to the shooting platforms and strategies. Next, a sparse point cloud was constructed. The software uses the Samantha algorithm, which is a sparse reconstruction technique based on multi-view analysis, recovering 3D structures by analyzing images from multiple camera

perspectives and building the sparse point cloud. The final step is to construct a dense point cloud, utilizing the 3DF Stasia algorithm, which excels at reconstructing details [37]. In addition to the above steps, to ensure that the distance between points in the dense point cloud corresponds to the actual distance, two points were marked on the pavement before taking the photos. The distance between these two points was 5 cm. After the reconstruction of the 3D model, the software's calibration function was used to scale the model to its real proportions.

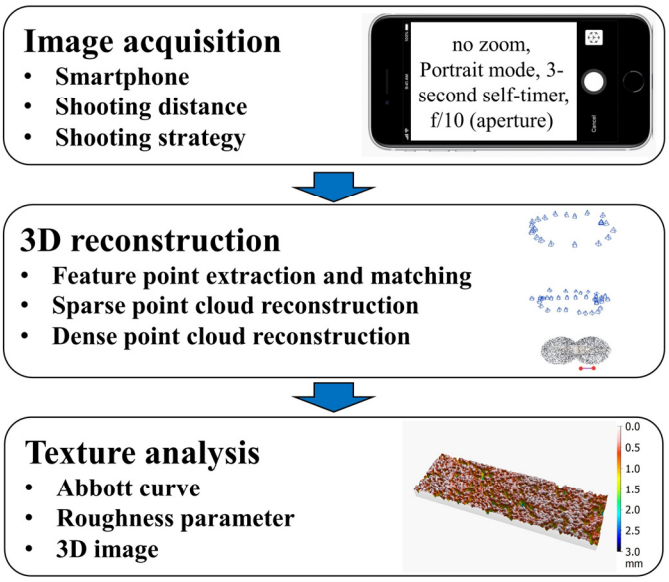

Figure 2. The overall workflow of CRP.

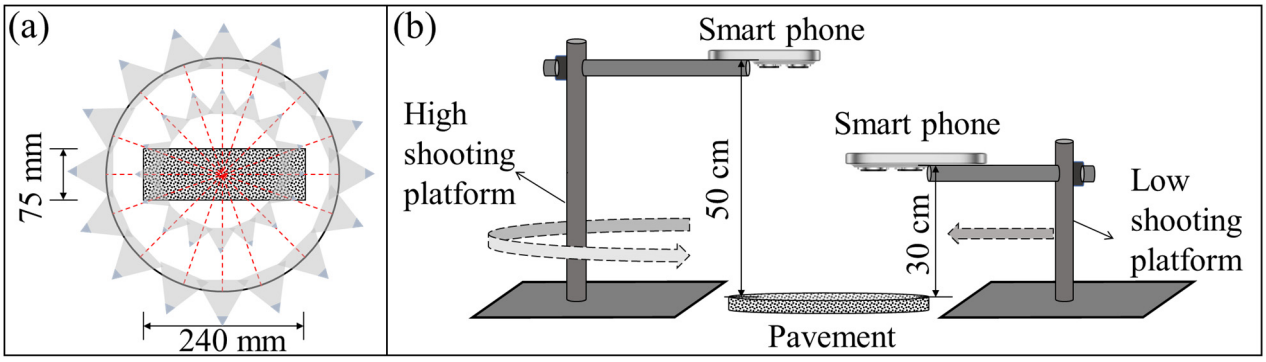

Figure 3. (**a**) Parallel axis capture; (**b**) Schematic diagram of the shooting platform.

Finally, texture analysis was performed based on the point cloud data obtained from the 3D reconstruction. In this study, the analysis was conducted using the software MountainsMap (v. 10.1). A series of operations were performed with this software, including rotation, cropping, leveling, and shape removal, to obtain the Abbott curve, roughness parameters, and 3D images of the road surface. The leveling process was handled using the least squares method. Subsequently, data obtained from structured light scanners and high-end cameras were analyzed using the software.

3.2. Photogrammetry Techniques Using High-End Reflex Camera

High-end camera photogrammetry technique is also a type of CRP, but the method of image acquisition differs, using more advanced cameras. In this study, a high-end reflex camera was used, featuring a CMOS sensor with dimensions of 36 × 24 mm, an image resolution of 5472 × 3648 pixels, and a pixel size of 6.54 µm, with an aperture value of

f/8. Both camera and sensor are manufactured by Canon Ink. (Tokyo, Japan). To ensure that the size of the reconstructed 3D images was more accurate and the results were better, coded targets were used in this study. The SfM software Agisoft Metashape (v. 2.1.2) was employed. The coded targets allowed computational optimization during reconstruction, leading to improved results. The coded targets, as shown in Figure 4, were placed in the scene before taking the photos and could be used as reference points for coordinate systems and scale definitions, or as effective matches between images. This method enhanced image quality by using a professional camera, and the introduction of coded targets improved the reconstruction results.

Figure 4. Example of an image acquired by the reflex camera and containing coded targets.

3.3. Structured-Light Projection Scanning

In this study, a structured-light scanner (SLS) was used to scan pavement textures and obtain point cloud data, which were then compared with the results from CRP based on the mobile phone. The structured-light scanner used in this study was the Artec Space Spider from Artec 3D (Senningerberg, Luxembourg), with detailed technical specs shown in Table 2. The scanner is shown in Figure 5a, and its point cloud results are shown in Figure 5b. Structured-light scanners emit a precisely calibrated blue or white light pattern. Typically, this pattern forms a set of parallel lines, stripes, or grids. When this "structured light" contacts the surface of the object, the light is distorted due to the surface's shape, with its depressions or protrusions. Simultaneously, the camera of the scanner captured the reflected light information frame by frame, recording the degree of distortion. By calculating these deformations, the 3D shape of the object was obtained, generating a 3D point cloud.

Table 2. Structured-light scanner technical specs.

Scanner Model	3D Accuracy	3D Resolution	3D Reconstruction Rate	Tracking Markers
Artec Space Spider	0.05 mm	0.1 mm	7.5 FPS	Markerless

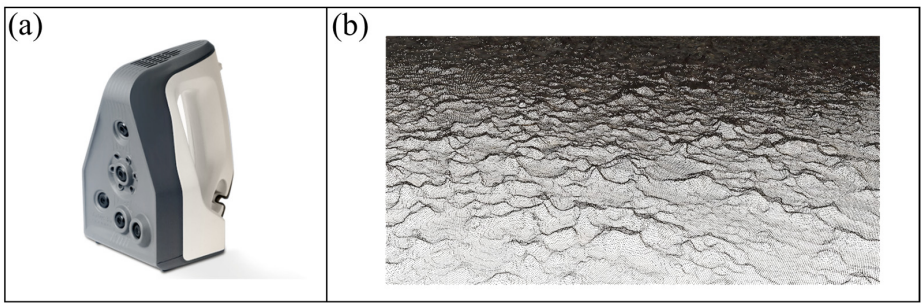

Figure 5. (**a**) The Structured-light scanner employed; (**b**) A 3D point cloud obtained.

3.4. Simulation of Contaminated Pavement

Hazardous liquid substance spills after road accidents can cause the chemical and structural decomposition of asphalt particles within the pavement texture. A study conducted by Girelli et al. emphasized that the longer the spilled substances remain on the road surface, the greater the damage assessed on the pavement texture [38]. Therefore, the timely removal of such substances from the road surface is of critical importance.

In this study, a contamination of the road surface by applying diesel, oil, and other pollutants was conducted and followed by a cleaning process. During the cleaning, sand was initially used to absorb the liquid contaminants, after which the surface was washed and air-dried, as shown in Figure 6. After cleaning, most of the sand was removed, but oil stains and water residues remained on the surface, creating a more complex texture condition. Under these conditions, various methods were employed to test the pavement texture in the same area to evaluate their performance in a challenging environment.

Figure 6. Image of pavement sweeping site.

4. Results and Discussion

4.1. The Effect of the Point Cloud Size on CRP Result Based on Mobile Phone

Typically, a higher number of elements in a point cloud corresponds to greater accuracy in the representation, which generally leads to better results. However, when photo resolution is limited, increasing accuracy through software will only increase point cloud sparsity and data processing complexity and amplify noise, without significantly improving measurement results, or even making the results worse. Because a large amount of error data or noise may be treated as correct information for texture evaluation, selecting an appropriate point cloud size is crucial. This study first analyzed the impact of various computational settings on point cloud data to determine the optimal sparsity settings. The software operation settings and point cloud sizes results are shown in Table 3. It can be observed that a different number of point clouds can be obtained through software settings, with the maximum size of point cloud data reaching 519,367, although the runtime is significantly longer than other tests. Comparing image resolution and acceleration levels shows that higher image resolution and lower acceleration levels led to more data points and a correspondingly longer runtime. For example, in Procedure B, with a high acceleration level and 100% resolution, the number of data points is 156,284. When the speed level is adjusted to low, the point cloud size reaches 5,139,367. When the resolution was adjusted to 75%, the number of data points dropped below 50,000, resulting in excessively low accuracy.

Table 3. Results of the point cloud size and software settings.

Procedure	Number of Points	Image Resolution	Speed Up Level	Running Time
A	80,308	50%	Low	2 m 24 s
B	156,284	100%	High	3 m 2 s
C	230,271	75%	Low	3 m 16 s
D	519,367	100%	Low	8 m 21 s

4.1.1. Results of Different Point Cloud Sizes Based Mobile Phone

The results of different size of point clouds are shown in Figure 7. It can be observed that, as the number of point cloud data elements increased, the point cloud more accurately reflected the surface details of the pavement. With the increase in the number of point cloud data points, the fine features and complex structures of the pavement can be better represented, and the color of the result also becomes more like the road surface. Comparing Procedure A and Procedure D in Figure 7, significant differences can be observed. The number of point clouds for Procedure A is the least, as fine surface details may be smoothed out or overlooked, resulting in the 3D model that may not accurately reflect the actual roughness of the pavement. This outcome can distort the calculated roughness value or cause critical roughness features to be missed. On the other hand, Procedure D had the highest number of elements in the point cloud, and the pavement texture can be reflected solely through the point cloud data. It is clear that high-resolution models were more detailed, and the generated 3D models would be closer to the real surface, although the computation time was longer. However, a roughness analysis should be compared using the Abbott curve and roughness parameters to quantify the impact of number of point clouds; the quality of CRP based on a mobile phone cannot be determined solely by point cloud models.

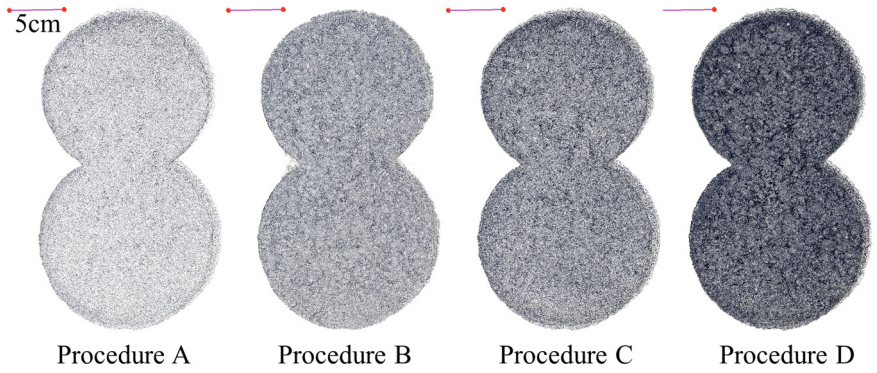

Figure 7. Results of dense point cloud from CRP technique based on mobile phone.

In this study, the point cloud results were processed, and a 240 mm × 75 mm area was selected for quantitative comparison with the scanner results of the same area. The cloud map results are shown in Figure 8. During texture calculation, the relevant software settings and procedures were kept completely consistent. It can be observed that the differences in the cloud map results due to variations in the number of points are not significant. However, Procedure D displays a finer texture effect, visually superior even to the scanner results, despite the scanner results containing more data points. This result may be due to the fact that the reconstruction process in Procedure D better reconstructs the details, but the correctness of the details is in doubt. Due to the presence of significant deep valleys in the pavement, these regions can be difficult to reconstruct from some angles due to lighting issues and to the absence of tilted photos that could capture the innermost areas. If the viewing angles are not diverse enough, some areas may lack information. In cases where high accuracy is required, the software often compensates through point interpolation algorithms, where the reconstruction algorithm might infer the shape and details of these

regions. This inference can make the result appear finer, potentially making it look better than the scanner results, but it may also lead to inaccurate results.

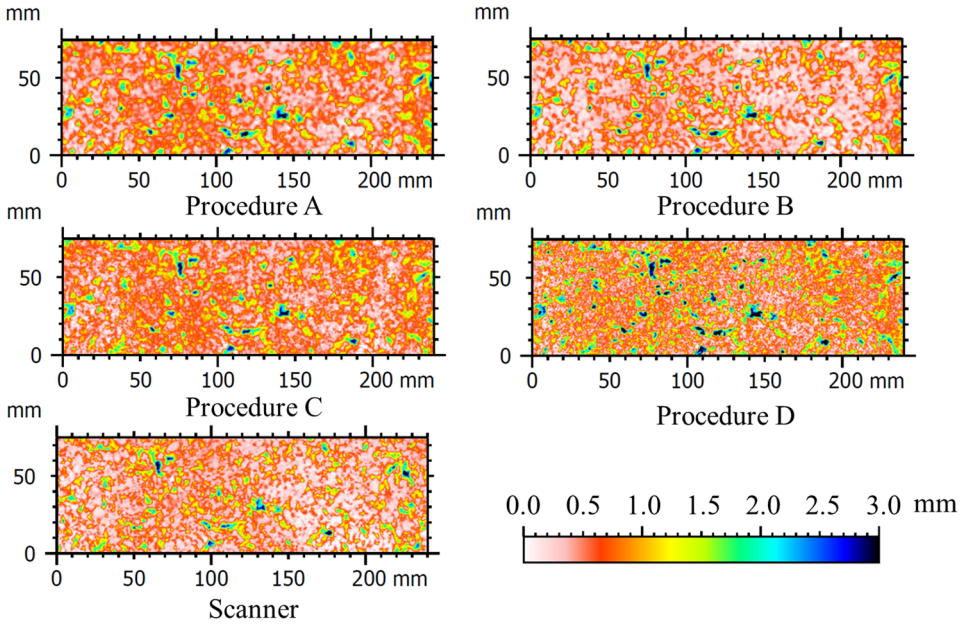

Figure 8. Cloud maps with different point cloud sizes and cloud maps from scanner.

4.1.2. The Effect of Point Clouds Size on Roughness and Abbot Curves

To quantify the impact of number of elements of the point cloud on pavement texture results, this study plotted the Abbott curves (Figure 9) and calculated the roughness parameters (Table 4), including the arithmetic mean height (*Sa*), root mean square height (*Sq*), maximum height (*Sz*), kurtosis (*Sku*), and skewness (*Ssk*). The roughness parameter calculation formula is shown in Equations (1)–(5). The Abbott curves show that changes in number of point clouds have a minimal effect on the differences from the scanner results. Even with the lowest number of point clouds, Procedure A, the results still performed well. Procedure B is most consistent with the scanner results, while the Abbott curve for Procedure D shows some deviation from the scanner results. This result may be due to the excessive inference of local details and an increase in the size of point cloud during the 3D reconstruction process, leading to distorted results. Additionally, high accuracy often comes with increased noise, resulting in the inclusion of more invalid points in the statistics, which affects the performance of the Abbott curve. The roughness parameter results show that the *Sa* and *Sq* values in Procedure D are significantly higher than in other groups, and, although there are some differences in *Ssk* and *Sku*, they remain within a reasonable range. *Sz* gradually becomes larger as the accuracy increases, which is supposed to be due to more noise. This finding further indicates that higher accuracy does not necessarily yield better results. Based on the above analysis, the settings used in Procedure B were adopted for subsequent CRP reconstructions in this study.

$$Sa = \frac{1}{A}\iint_A |Z(x,y)|dxdy \quad (1)$$

$$Sq = \sqrt{\frac{1}{A}\iint_A |Z^2(x,y)|dxdy} \quad (2)$$

$$Sz = Sp + Sv \quad (3)$$

$$Sku = \frac{1}{Sq^4}\left[\frac{1}{A}\iint_A \left|Z^4(x,y)\right|dxdy\right] \quad (4)$$

$$Ssk = \frac{1}{Sq^3}\left[\frac{1}{A}\iint_A \left|Z^3(x,y)\right|dxdy\right] \quad (5)$$

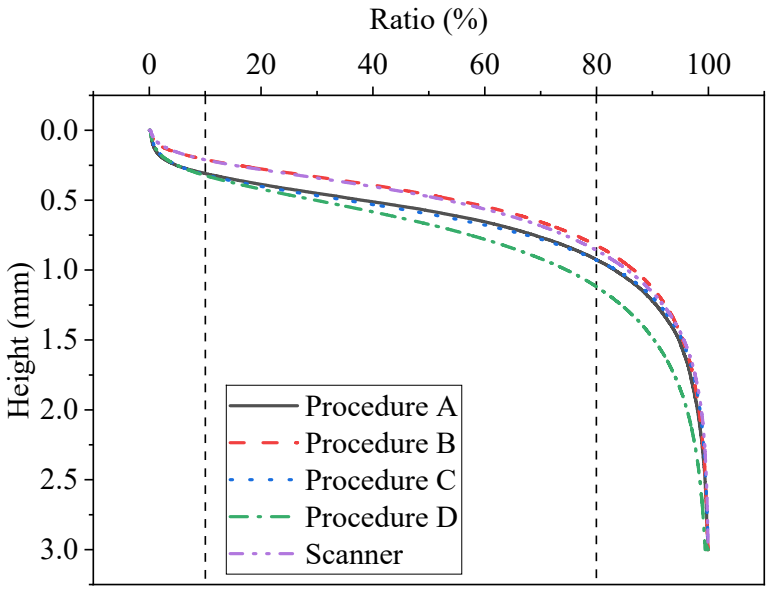

Figure 9. Abbott curves from different point cloud sizes and from the scanner.

Table 4. Roughness parameters from different point cloud sizes and from the scanner.

Procedure	Sa (mm)	Sq (mm)	Sz (mm)	Ssk	Sku
A	0.303	0.4237	3.947	−1.967	8.516
B	0.3092	0.4334	4.084	−2.098	9.238
C	0.2892	0.4012	4.021	−1.829	8.194
D	0.382	0.5257	5.160	−1.86	8.169
Scanner	0.3116	0.4208	3.221	−1.75	7.110

4.2. Comparison of Results for Different Texture Assessment Techniques

4.2.1. Comparison of Abbott Curves for Different Texture Assessment Techniques

In this study, five representative locations on a newly paved road were selected for texture analysis with the three methods (CRP with mobile phone, CRP with professional camera, and Scanner), and Abbott curves were plotted based on the collected point cloud data, as shown in Figure 10. The results indicate that, with the exception of Location 4, the Abbott curves from different methods are generally consistent. For Location 4, the Abbott curves from the scanner and the professional camera are fairly consistent, while the curve derived from the mobile phone shows significant differences. This result suggests that, although CRP based on a mobile phone offers a low-cost solution, its accuracy in road pavement texture detection may be limited. In contrast, CRP using high-end cameras proves to be more reliable, with results comparable to those obtained by the scanner.

Further analysis of the Abbott curves reveals that points corresponding to a texture height of 0–0.7 mm constitute over 50% of the total, with some pavement locations reaching up to 80%, indicating that the surfaces are relatively flat. This finding can be attributed to the fact that the maximum aggregate size is only 12.5 mm, and the road is newly constructed, resulting in high smoothness. When the pavement texture height is low, the Abbott curves obtained by different methods closely overlap. However, as the texture

height increases, significant discrepancies occur among the curves. This trend indicates that, while different methods perform well in capturing shallow pavement textures, they exhibit varying effectiveness when detecting deeper textures. This discrepancy may be due to the challenges in capturing points at greater depths on pavement. Therefore, future research should focus on improving the detection of deeper pavement textures and optimizing CRP based on a mobile phone to enhance its reliability.

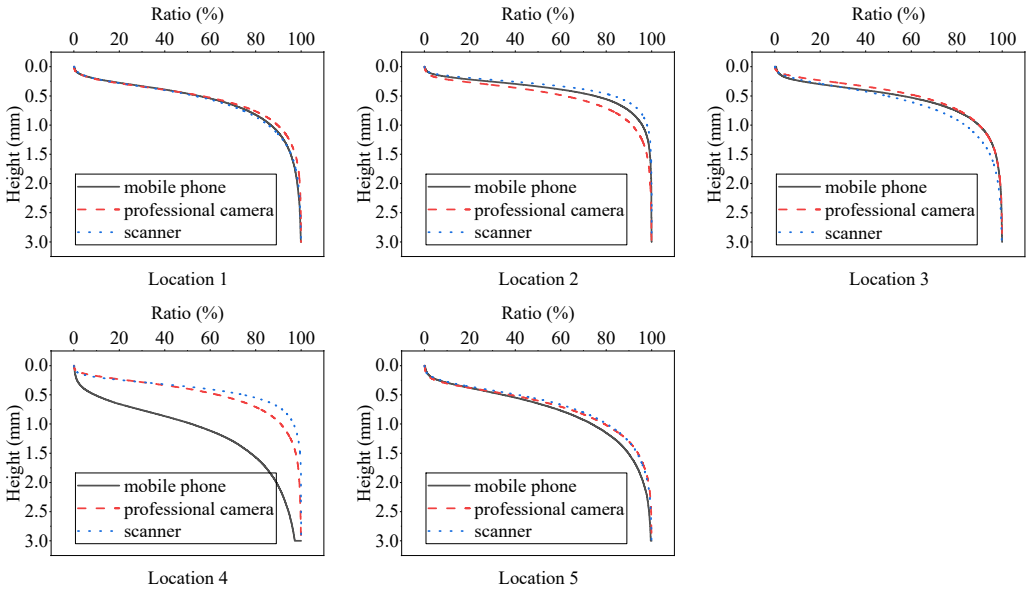

Figure 10. Abbott curves for results of different methods in five locations.

4.2.2. Comparison of Roughness Parameters for Different Texture Assessment Techniques

This study calculated the roughness parameters at five locations with the results shown in Figure 11. Comparing the height distribution parameters *Sa*, *Sq*, and *Sz*, the differences between the results from different methods are minimal, except for Location 4. This outcome further confirms the feasibility of CRP methods for pavement texture detection. Specifically, *Sa* values range from 0.1 to 0.4 mm, *Sq* values range from 0.1 to 0.6 mm, and *Sz* values are around 4 mm, indicating that the roughness at different locations is relatively consistent, because the road has just been paved and is quite smooth. For Location 4, the roughness parameters obtained using a mobile phone are significantly higher than those obtained using other methods, possibly due to the deeper texture at that location, which makes it difficult for the mobile phone's CRP to accurately capture the depth information. This action would overestimate the pavement texture depth. In contrast, the professional camera performs well, likely because its larger CMOS sensor can capture faint light better, while the mobile phone's smaller sensor and lower resolution result in less detailed images, leading to reduced reconstruction accuracy.

When comparing the *Sku* and *Ssk* parameters, the differences among the five locations across different methods are minimal. Even at Location 4, the results from the mobile phone, professional camera, and scanner are generally consistent. The *Sku* values are all greater than three, indicating that the height distribution is more peaked. Typically, $Sku = 3$ suggests a normal distribution, while $Sku > 3$ indicates a sharper height distribution. This may be due to the fact that the asphalt concrete has recently been laid, and the aggregate has not yet worn down, resulting in sharp texture. The *Ssk* values are all less than 0; typically, $Ssk = 0$ indicates that the height distribution of the pavement texture is symmetrical, while $Ssk < 0$ suggests that the texture distribution is skewed upwards. The results show that the pavement texture is indeed skewed upwards, consistent with the Abbot curve analysis, where the curve changes rapidly at low texture heights. Overall, these findings indicate that the pavement roughness data obtained by CRP methods are reliable and can effectively reflect the pavement texture.

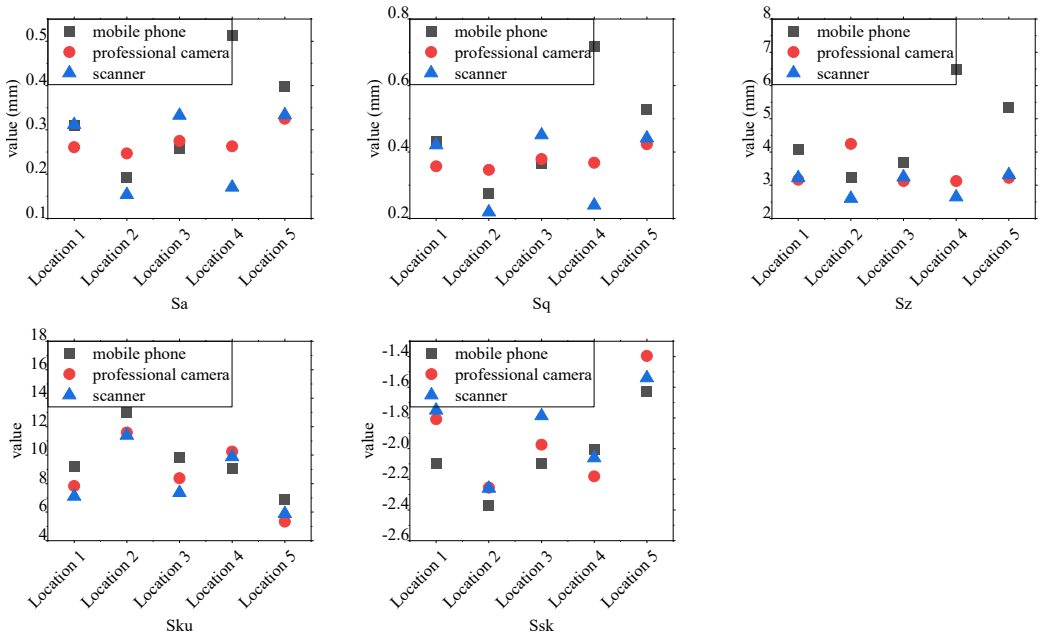

Figure 11. Roughness parameters for different locations.

4.2.3. Comparison of Cloud Maps for Different Locations

To investigate the reasons for inaccuracies in results based on mobile phone image reconstruction, this study compared the point cloud results from five locations, as shown in Figure 12. The results indicate that the point cloud at Location 4 is distinctly different from the other four locations. Location 4 has deeper textures with many deep valleys, some of which exceed 3.0 mm in depth. These deep valleys are likely the cause of the decreased accuracy that CRP based on the mobile phone. Due to the lower resolution of mobile phone images and the reduced light reflection in deep valley areas, the mobile phones struggle to accurately capture the height variations in these regions. When reconstructing the three-dimensional structure of the pavement surface based on mobile images, this action inevitably leads to fewer point cloud data in these areas and even reconstruction errors, where deep valleys are misjudged as being deeper than they actually are, resulting in an overestimation of pavement roughness.

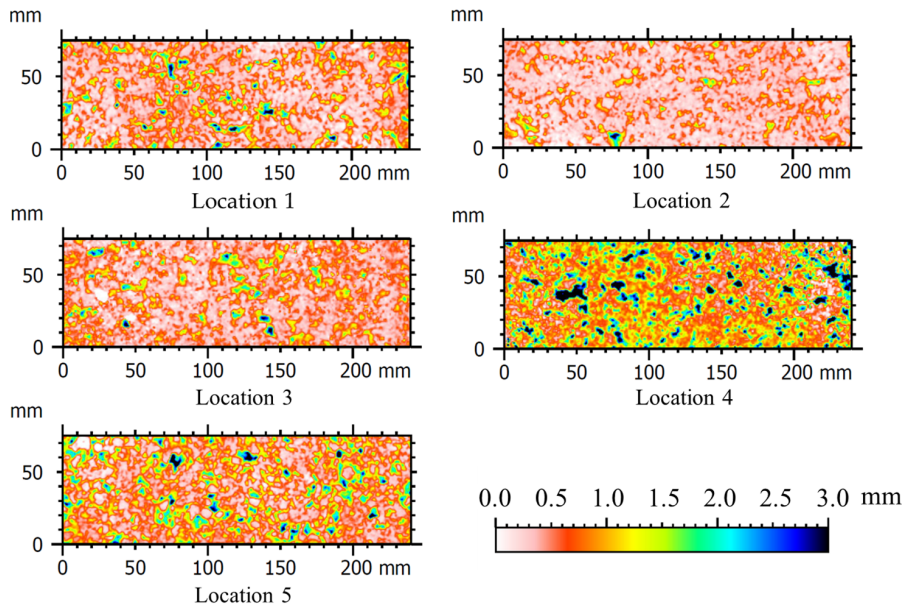

Figure 12. The results of cloud maps at different locations by CRP based on mobile phone.

The pavement surface at Location 5 is also relatively rough, but the three-dimensional reconstruction is more accurate. This finding may be because, although Location 5 has many valleys, they are not very deep. The blue and black areas are significantly fewer than in Location 4, and more areas are shown in blue, indicating that the depth is within 3 cm. Therefore, the CRP based on the mobile phone is still feasible in this case. The other three locations have noticeably flatter pavement surfaces, and the method images are sufficient to reflect the roughness, with reconstruction results closely matching those from the scanner. In summary, the CRP based on mobile phone technology is more suitable for pavement surfaces with smaller roughness and fewer deep valleys. For pavements with numerous deep valleys, the reliability of the results obtained using this method should be carefully assessed.

This observation was also confirmed by another test conducted to compare the outcomes obtained with the tested methods. The five different point clouds, for all the test areas considered, were imported in the free software for point cloud processing CloudCompare, and a cloud-to-cloud distance calculation was performed using as a reference the SLS cloud, to which the mobile-phone CRP clouds were compared. This operation allows us to understand the distribution of the inter-distance between the points of two aligned clouds, selecting a distance range and also a direction along which to compare the points (X, Y, or Z). In this case, the point inter-distance was first computed along the X and Y axis, not showing significative differences among the clouds obtained with the three devices. Then, the distances along the Z axis were calculated to compare the points representing the depth, hence understanding the differences in the reconstruction of the innermost areas among the two surveying techniques (scanner vs. mobile phone).

The Z value differences ranged from −5.24 mm to +2.40 mm, with the worst-case being Location 4, confirming what was mentioned above. The best situation, instead, was observed for Location 1 (−1.49 mm to +0.88 mm). Table 5 reports the results obtained for each test area, while Figure 13 shows the mobile phone-based point cloud of Location 4, represented with a color gradient showing the differences in the distance values (in mm) in the Z direction. As mentioned before, the innermost areas in the aggregate concavities present points with a significant discrepancy in the Z values between the two surveying techniques. This finding demonstrates again that mobile-phone photogrammetry is more suitable for shallow surfaces, as it is not sufficiently able to reconstruct the innermost and hard-to-capture areas of the aggregate. The SLS, instead, despite presenting some problems with the wet and oiled surfaces after spilling, was more able to "penetrate" inside the most hidden morphological features of the scanned areas.

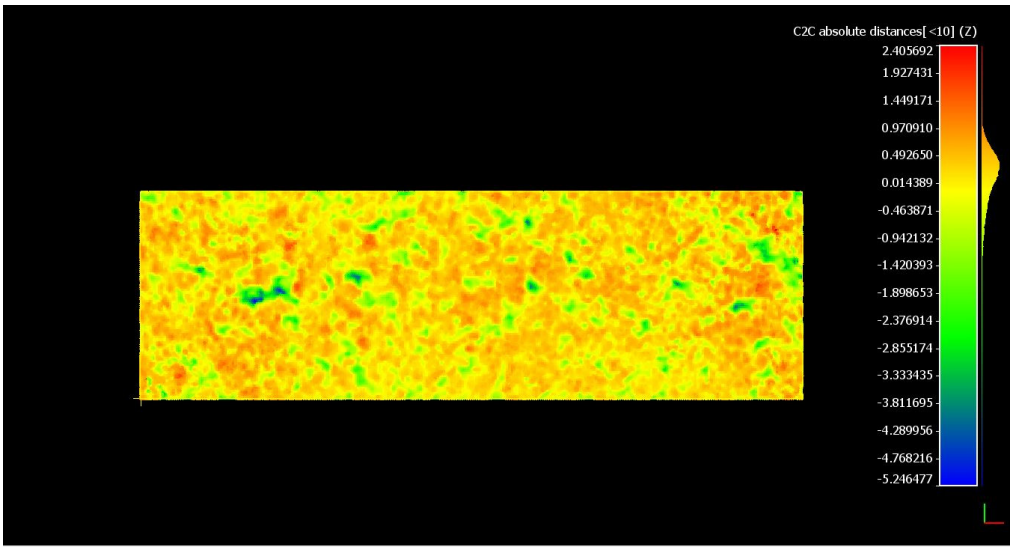

Figure 13. Mobile phone point cloud of Location 4, represented with a color gradient showing the Z values (in mm) differences concerning the cloud scanned with SLS.

Table 5. Distance values differences in the Z direction for all the test areas considered (mobile phone vs. structured-light scanner).

Location	Z Values Distances (min–max) with Respect to the SLS Scanned Clouds
1	−1.49 (min) +0.88 (max)
2	−2.82 (min) +1.52 (max)
3	−3.05 (min) +1.92 (max)
4	−5.24 (min) +2.40 (max)
5	−2.56 (min) +1.01 (max)

4.3. Effects of Pavement Contamination on Results

To investigate the performance of CRP in complex environments, this study conducted texture measurements on four samples with small amounts of oil and water stains, and the point cloud results are shown in Figure 14. It can be seen that the CRP based on images was able to capture the pavement textures in these areas completely, whereas the three sets of data obtained using the scanner were incomplete. Comparing the details, it is evident that the scanner results in some areas differ significantly from the point cloud data obtained by other methods, which may be due to two factors. First, the structured- light scanner relies on projecting stripes or patterns to measure the surface of objects, making the quality and stability of the light source crucial. The bright daylight environment may have interfered with the operation. Second, the high reflectivity of the oil and water stains on the pavement surface could have caused intense specular reflection, making it difficult for the camera to accurately capture the stripes or patterns, leading to incomplete areas in the point cloud results. This finding demonstrates that, although the scanner offers high precision, its effectiveness can be compromised in complex environments, potentially resulting in distorted data and difficulties in detecting certain areas.

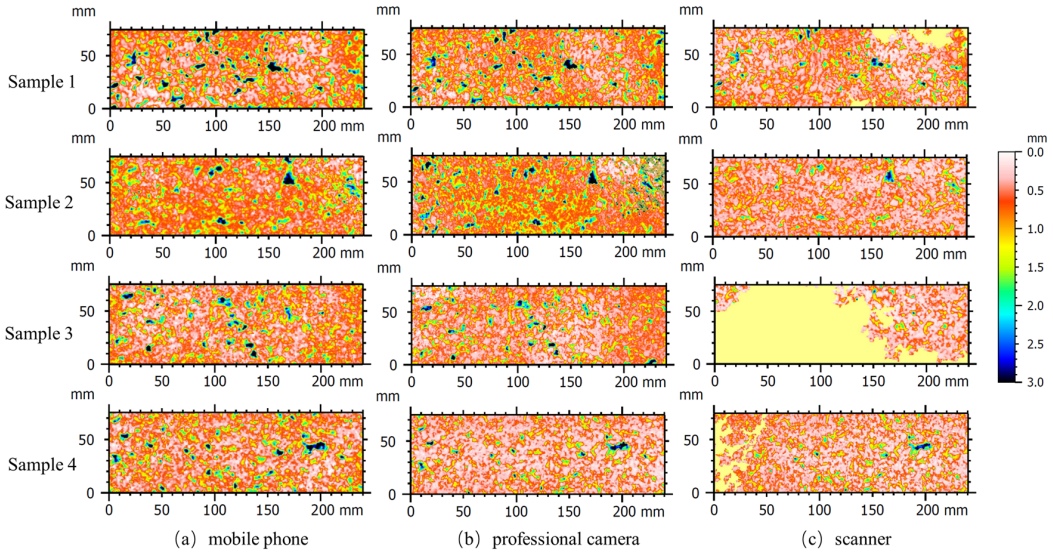

Figure 14. The results of cloud maps in case of contamination.

To further analyze the impact of environmental factors on pavement texture detection, this study conducted a statistical analysis of the point cloud results and plotted Abbott curves, as shown in Figure 15. The Abbott curves obtained from different testing methods are generally similar, with some curves even nearly overlapping. However, there are also some differences, particularly with the Abbott curve from the scanner, which is relatively higher than those from the other two methods. This discrepancy may be related to the incompleteness of the scanner data. Even in the case where the scanner data are complete, as

shown in Figure 15 (Sample 2), the Abbott curve remains higher than that obtained through CRP, indicating that the presence of water on the road surface may impact the scanner's accuracy, leading to deviations in the results. Therefore, even when the scanned area is complete, the authenticity of the data needs further validation in complex environments.

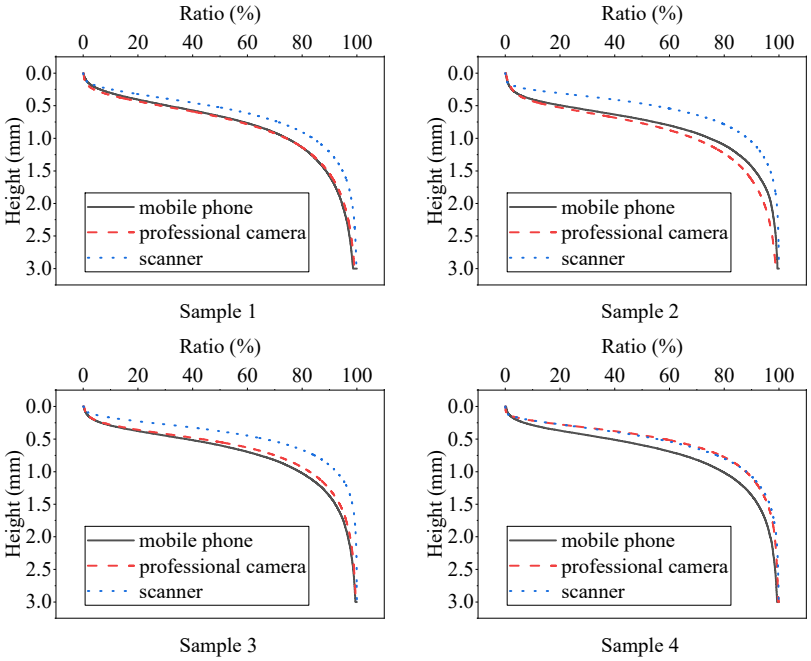

Figure 15. Abbott curves for results of different methods of four samples.

This study calculated pavement roughness based on point cloud data, with the results shown in Figure 16. Comparing the parameters *Sa*, *Sq*, and *Sz*, it is evident that the results obtained from the scanner are consistently lower than CRP methods. The CRPs based on mobile phone and professional camera measurement results are more closely aligned, indicating that, in the presence of water, the scanner may primarily capture shallower areas, while deeper valleys, affected by the water, are either difficult to scan or experience distortion due to the adverse effects on structured light. This result leads to an underestimation of the pavement roughness. The *Sku* values are all greater than 3, and *Ssk* values are all less than 0, indicating that the pavement surface remains relatively sharp, with the overall point cloud distribution skewed upward. When comparing *Sku* and *Ssk* values across different methods, there is a noticeable increase in dispersion compared to tests conducted on dry pavement surfaces. This finding indicates that the presence of water impacts the testing results, leading to some variation between the methods used.

These findings indicate that, while scanners offer high precision, CRP may have an advantage in pavement surface reconstruction under certain conditions, particularly when contaminants or strong lighting are present. To address such issues, many high-precision scanners on the market today are designed as hybrid systems, incorporating both structured-light emitters and cameras. This design allows them to generate 3D point clouds through structured-light scanning and simultaneously capture 3D structures through imaging techniques, ultimately optimizing and merging the two results for a more accurate representation of the scanned object. This outcome demonstrates that, although CRP is not as precise as scanning, it may offer distinct advantages in specific scenarios and can be more efficient in the field since it only requires taking photographs, making it faster than using a scanner.

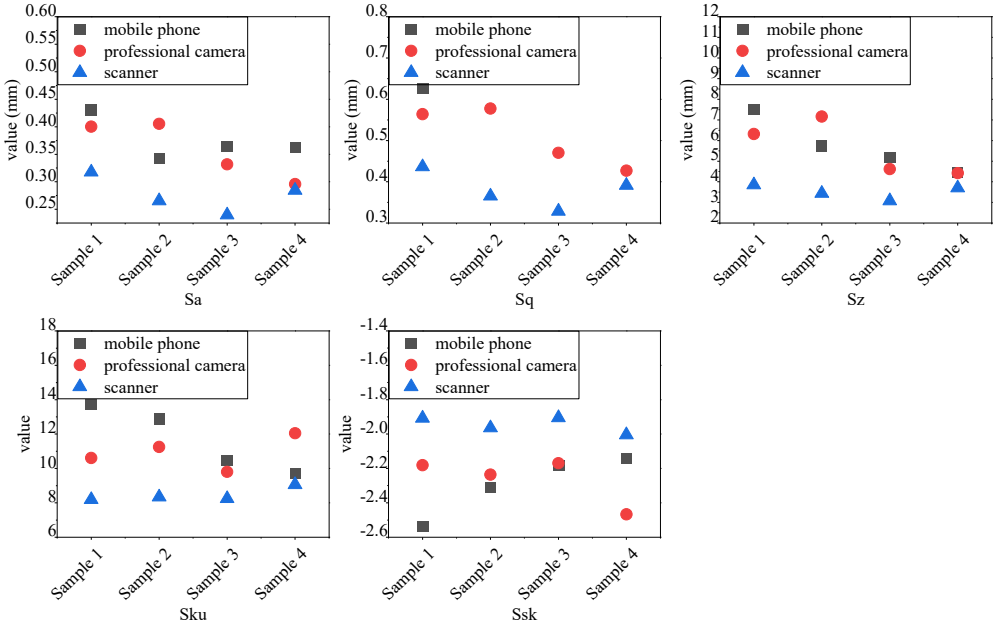

Figure 16. Roughness parameters for different locations in case of contamination.

5. Conclusions

This study introduces a CRP technique based on mobile phone images, firstly analyzing the effect of the number of point clouds on the texture image, the Abbott curve, and the roughness parameters. Then, it compares the differences in pavement texture reconstruction results between a mobile phone, professional camera, and structured-light scanners. Finally, this study assesses the effects of water presence and contamination on these three testing methods. Based on the comprehensive analysis and comparison, the following conclusions can be drawn:

(1) The CRP technique using mobile phone images can effectively detect pavement textures, and, through photogrammetric expertise and practice, algorithmic adjustments and software settings can produce high-precision 3D point cloud results. However, too many points can affect the authenticity of the pavement texture. While more points would better reflect the details of the pavement, it may also introduce noise and redundant information, leading to distorted results. Abbott curves and roughness parameters may vary with changes in accuracy, indicating that an increased number of points does not always result in more precise measurements. Therefore, selecting an appropriate setting is crucial.

(2) The Abbott curves and roughness parameters obtained by different detection methods are generally consistent, indicating that these methods perform well in detecting shallow pavement textures. However, the CRP technique based on mobile phones struggles with deep texture detection due to lower image resolution and insufficient light capture in deep valleys. This challenge affects the 3D reconstruction and leads to an overestimation of roughness on surfaces with significant valleys. Hence, this technique is more suitable for analyzing textures on flat surfaces, and caution is advised when evaluating its accuracy on complex surfaces.

(3) Although scanners typically offer greater accuracy than CRP, this study found that, in environments with water and oil presence, scanners are more susceptible to the effects of light and surface reflections, leading to incomplete or distorted data. In contrast, close-range photogrammetry demonstrates a greater advantage under such conditions, capturing pavement details more completely. This technique exhibits better adaptability in complex environments and holds specific advantages under certain conditions.

In terms of sustainability, this study presents a method for rapid and cost-effective assessments of road pavement surface conditions. Compared to traditional methods for analyzing road pavements after a maintenance event, the proposed method is more economically sustainable. This property is primarily due to its expedited nature, which significantly reduces the time required for road closures compared to traditional, point-based, and static testing methods. Additionally, the method is cost-effective because it utilizes a simple mobile phone equipped with a camera, allowing the acquisition of data that is comparable in quality to that obtained with more expensive equipment. The proposed methodology also offers greater environmental sustainability by minimizing waste production and reducing the overall waste management burden. Moreover, if the pavement is found to be inadequate in terms of functional parameters, the method allows for a rapid and targeted plan for reusing the bituminous mixture that needs to be removed, further contributing to resource efficiency.

Further studies will be conducted on different types of pavements, with enhanced control over factors that may interfere with image acquisition.

Author Contributions: Conceptualization, M.P., V.V. and C.L.; methodology, C.L., M.B. and A.F.; software, Z.G., M.B. and A.F.; data curation, M.B., Z.G. and C.L.; writing, Z.G., M.B. and M.P.; validation, V.V., M.P. and V.A.G.; supervision, C.L. All authors have read and agreed to the published version of the manuscript.

Funding: This research received no external funding.

Institutional Review Board Statement: Not applicable.

Informed Consent Statement: Not applicable.

Data Availability Statement: Data are contained within this article.

Acknowledgments: This study was carried out within the Spoke 7 of the MOST—Sustainable Mobility National Research Center and received funding from the European Union Next-GenerationEU (PIANO NAZIONALE DI RIPRESA E RESILIENZA (PNRR)—MISSIONE 4 COMPONENTE 2, INVESTIMENTO 1.4—D.D. 1033 17/06/2022, CN00000023). This manuscript reflects only the authors' views and opinions. Neither the European Union nor the European Commission can be considered responsible for them. The authors would like also to thank the company Zini Elio srl for its support in providing materials for this research and the 'Autodromo Enzo e Dino Ferrari' International Circuit for providing the field trial site.

Conflicts of Interest: The authors declare no conflicts of interest.

References

1. Chen, S.; Liu, X.; Luo, H.; Yu, J.; Chen, F.; Zhang, Y.; Ma, T.; Huang, X. A State-of-the-Art Review of Asphalt Pavement Surface Texture and its Measurement Techniques. *J. Road Eng.* **2022**, *2*, 156–180. [CrossRef]
2. Karen, İ.; Kaya, N.; Öztürk, F.; Korkmaz, İ.; Yıldızhan, M.; Yurttaş, A. A Design Tool to Evaluate the Vehicle Ride Comfort Characteristics: Modeling, Physical Testing, and Analysis. *Int. J. Adv. Manuf. Technol.* **2012**, *60*, 755–763. [CrossRef]
3. Bueno, M.; Luong, J.; Terán, F.; Viñuela, U.; Paje, S.E. Macrotexture Influence On Vibrational Mechanisms of the Tyre–Road Noise of an Asphalt Rubber Pavement. *Int. J. Pavement. Eng.* **2013**, *15*, 606–613. [CrossRef]
4. Wang, C.; Wang, M.; Xiao, X.; Guo, J. Preparation and Evaluation of Durability of Color Antiskid Pavement Particles Subjected to Different Treatments. *J. Mater. Civ. Eng* **2020**, *32*, 4019336. [CrossRef]
5. Zheng, B.; Chen, J.; Zhao, R.; Tang, J.; Tian, R.; Zhu, S.; Huang, X. Analysis of Contact Behaviour On Patterned Tire-Asphalt Pavement with 3-D FEM Contact Model. *Int. J. Pavement. Eng.* **2022**, *23*, 171–186. [CrossRef]
6. Peng, Y.; Li, J.Q.; Zhan, Y.; Wang, K.C.P.; Yang, G. Finite Element Method-Based Skid Resistance Simulation Using in-Situ 3D Pavement Surface Texture and Friction Data. *Materials* **2019**, *12*, 3821. [CrossRef]
7. Bitelli, G.; Simone, A.; Girardi, F.; Lantieri, C. Laser Scanning On Road Pavements: A New Approach for Characterizing Surface Texture. *Sensors* **2012**, *12*, 9110–9128. [CrossRef]
8. Zheng, B.; Tang, J.; Chen, J.; Zhao, R.; Huang, X. Investigation of Adhesion Properties of Tire—Asphalt Pavement Interface Considering Hydrodynamic Lubrication Action of Water Film On Road Surface. *Materials* **2022**, *15*, 4173. [CrossRef]

9. Ren, W.; Han, S.; Fwa, T.F.; Zhang, J.; He, Z. A New Laboratory Test Method for Tire-Pavement Noise. *Measurement* **2019**, *145*, 137–143. [CrossRef]
10. Wei, S.; Wang, Y.; Cheng, H.; Wang, D. Stress Distributions in the Textures of Prefabricated Pavement Surface Created with the Assistance of 3D Printing Technology. *Int. J. Pavement. Eng.* **2021**, *24*, 1–17. [CrossRef]
11. Jain, S.; Das, A.; Venkatesh, K.S. Automated and Contactless Approaches for Pavement Surface Texture Measurement and Analysis—A Review. *Constr. Build. Mater.* **2021**, *301*, 124235. [CrossRef]
12. Wang, W.; Yan, X.; Huang, H.; Chu, X.; Abdel-Aty, M. Design and Verification of a Laser Based Device for Pavement Macrotexture Measurement. *Transp. Res. Part C Emerg. Technol.* **2011**, *19*, 682–694. [CrossRef]
13. Ech, M.; Yotte, S.; Morel, S.; Breysse, D.; Pourteau, B. Laboratory Evaluation of Pavement Macrotexture Durability. *Rev. Eur. De Génie Civ.* **2007**, *11*, 643–662. [CrossRef]
14. Gong, Z.; Miao, Y.; Li, W.; Yu, W.; Wang, L. Analysis of Tyre-Pavement Contact Behaviour of Heavy Truck in Full-Scale Test. *Int. J. Pavement. Eng.* **2023**, *24*, 2235630. [CrossRef]
15. Wang, H.; Ma, J.; Yang, H.; Sun, F.; Wei, Y.; Wang, L. Development of Three-Dimensional Pavement Texture Measurement Technique Using Surface Structured Light Projection. *Measurement* **2021**, *185*, 110003. [CrossRef]
16. Luhmann, T. Close Range Photogrammetry for Industrial Applications. *Isprs J. Photogramm.* **2010**, *65*, 558–569. [CrossRef]
17. Simone, A.; Lantieri, C.; Vignali, V.; Bitelli, G.; Girardi, F. 3D Laser Scanner Technique for in Situ Analysis of Road Pavement Surface Texture. In Proceedings of the 7th International Conference on Maintenance and Rehabilitation of Pavements and Technological Control, Auckland, New Zealand, 28–30 August 2012.
18. Dondi, G.; Simone, A.; Vignali, V.; Lantieri, C. Characterization of Pavement Surface Texture Using 3D Laser Scanner Technique. In Proceedings of the 11th International Conference on Asphalt Pavement, Nagoya, Aichi, Japan, 1–6 August 2010.
19. Miao, Y.; Wu, J.; Hou, Y.; Wang, L.; Yu, W.; Wang, S. Study On Asphalt Pavement Surface Texture Degradation Using 3-D Image Processing Techniques and Entropy Theory. *Entropy* **2019**, *21*, 208. [CrossRef] [PubMed]
20. Balzani, R.; Barzaghi, S.; Bitelli, G.; Bonifazi, F.; Bordignon, A.; Cipriani, L.; Colitti, S.; Collina, F.; Daquino, M.; Fabbri, F.; et al. Saving Temporary Exhibitions in Virtual Environments: The Digital Renaissance of Ulisse Aldrovandi—Acquisition and Digitisation of Cultural Heritage Objects. *Digit. Appl. Archaeol. Cult. Herit.* **2024**, *32*, e00309. [CrossRef]
21. Li, L.; Wang, K.C.P.; Li, Q.J. Geometric Texture Indicators for Safety On AC Pavements with 1Mm 3D Laser Texture Data. *Int. J. Pavement Res. Technol.* **2016**, *9*, 49–62. [CrossRef]
22. Kováč, M.; Brna, M.; Pisca, P.; Jandačka, D.; Decký, M. The Influence of Road Pavement Materials On Surface Texture and Friction. *Sustainability* **2023**, *15*, 12195. [CrossRef]
23. Saif, W.; Alshibani, A. Smartphone-Based Photogrammetry Assessment in Comparison with a Compact Camera for Construction Management Applications. *Appl. Sci.* **2022**, *12*, 1053. [CrossRef]
24. Li, S.; Zhao, X.; Zhou, G. Automatic Pixel-Level Multiple Damage Detection of Concrete Structure Using Fully Convolutional Network. *Comput. Aided Civ. Inf.* **2019**, *34*, 616–634. [CrossRef]
25. Fang, K.; Dong, A.; Tang, H.; Miao, M.; An, P.; Zhang, B.; Jia, S. 3D Tunnel Reconstruction and Visualization through Multi-Smartphone Photogrammetry. *Measurement* **2023**, *223*, 113764. [CrossRef]
26. Fang, K.; Dong, A.; Tang, H.; An, P.; Wang, Q.; Jia, S.; Zhang, B. Development of an Easy-Assembly and Low-Cost Multismartphone Photogrammetric Monitoring System for Rock Slope Hazards. *Int. J. Rock. Mech. Min.* **2024**, *174*, 105655. [CrossRef]
27. An, P.; Tang, H.; Li, C.; Fang, K.; Lu, S.; Zhang, J. A Fast and Practical Method for Determining Particle Size and Shape by Using Smartphone Photogrammetry. *Measurement* **2022**, *193*, 110943. [CrossRef]
28. Wan, T.; Wang, H.; Feng, P.; Diab, A. Concave Distribution Characterization of Asphalt Pavement Surface Segregation Using Smartphone and Image Processing Based Techniques. *Constr. Build. Mater.* **2021**, *301*, 124111. [CrossRef]
29. Slavkovic, N.; Bjelica, M. Risk Prediction Algorithm Based On Image Texture Extraction Using Mobile Vehicle Road Scanning System as Support for Autonomous Driving. *J. Electron. Imaging* **2019**, *28*, 1. [CrossRef]
30. Farhadmanesh, M.; Cross, C.; Mashhadi, A.H.; Rashidi, A.; Wempen, J. Highway Asset and Pavement Condition Management Using Mobile Photogrammetry. *Transp. Res. Rec. J. Transp. Res. Board* **2021**, *2675*, 296–307. [CrossRef]
31. Kogbara, R.B.; Masad, E.A.; Kassem, E.; Scarpas, A.T. Skid Resistance Characteristics of Asphalt Pavements in Hot Climates. *J. Transp. Eng. Part B Pavements* **2018**, *144*, 4018015. [CrossRef]
32. Dong, S.; Han, S.; Wu, C.; Xu, O.; Kong, H. Asphalt Pavement Macrotexture Reconstruction From Monocular Image Based On Deep Convolutional Neural Network. *Comput. Aided Civ. Inf.* **2022**, *37*, 1754–1768. [CrossRef]
33. Pranjić, I.; Deluka-Tibljaš, A. Pavement Texture–Friction Relationship Establishment Via Image Analysis Methods. *Materials* **2022**, *15*, 846. [CrossRef] [PubMed]
34. Tian, X.; Xu, Y.; Wei, F.; Gungor, O.; Li, Z.; Wang, C.; Li, S.; Shan, J. Pavement Macrotexture Determination Using Multi-View Smartphone Images. *Photogramm. Eng. Remote Sens.* **2020**, *86*, 643–651. [CrossRef]
35. Dabove, P.; Grasso, N.; Piras, M. Smartphone-Based Photogrammetry for the 3D Modeling of a Geomorphological Structure. *Appl. Sci.* **2019**, *9*, 3884. [CrossRef]
36. Toldo, R.; Gherardi, R.; Farenzena, M.; Fusiello, A. Hierarchical Structure-and-Motion Recovery From Uncalibrated Images. *Comput. Vis. Image Underst.* **2015**, *140*, 127–143. [CrossRef]

37. Toldo, R. Towards Automatic Acquisition of High-Level 3D Models from Images. Ph.D. Thesis, Università Degli Studi di Verona, Verona, Italy, 2013.
38. Girelli, V.A.; Cotignoli, L.; Ghasemi, N.; Lantieri, C.; Tini, M.A.; Vecchione, R.; Bitelli, G.; Vignali, V. Assessing Hazardous Spills Impact On Road Surface Performances by 3D High Resolution Surveying Techniques. In Proceedings of the International Conference on Trends on Construction in the Post-Digital Era, Guimarães, Portugal, 7–9 September 2022.